Electronic Supplementary Information (ESI)

Controllable Synthesis of Single Crystalline Sn-based Oxides and Their Application to Perovskite Solar Cells

Eun Joo Yeom[ab]†, Seong Sik Shin[ac]†, Woon Seok Yang[d], Seon Joo Lee[a], Wenping Yin[b], Dasom Kim[b], Jun Hong Noh[a], Tae Kyu Ahn[*b], and Sang Il Seok[*ad]

[a]Division of Advances Materials, Korea Research Institute of Chemical Technology, Daejeon 34114, Korea

[b]Department of Energy Science, Sungkyunkwan University, Suwon 16419, Korea

[c]Department of Mechanical Engineering, Massachusetts Institute of Technology, Cambridge 02139, USA

[d]Energy and Chemical Engineering, UNIST, Ulsan 44919, Korea

Experiment

Synthesis of Sn based nanostructures.

The Sn based nanostructures with varying Zn concentration (x=0, 0.3, 1.0, 1.8, 2) were prepared using a conventional hydrothermal method. All the chemicals used here were of regent grade without further purification. In brief, 0.064 mmol tin tetrachloride ($SnCl_4 \cdot 5H_2O$, Aldrich) and appropriate amount of zinc chloride ($ZnCl_2 \cdot 2H_2O$, Aldrich) were dissolved in deionized water (300 ml) under vigorous magnetic stirring. Then, hydrazine monohydrate ($N_2H_4 \cdot H_2O$, Aldrich) was added dropwise into the reaction solution. The white precipitates formed immediately, after 20 min, the solution including the precipitate was transferred to Teflon-lined autoclave and kept at 220 ^oC for 12h. The obtained products were thoroughly collected by centrifugation and washed with deionized water and ethanol for several times. Finally, the products were dispersed in 2-methoxy ethanol.

Characterization.

The crystalline structures of Sn based materials were examined using a XRD (New D8 Advance, Bruker) with Cu K_α (λ = 0.154 nm). The morphologies and microstructures of the samples were investigated by field emission scanning electron microscopy (FESEM, SU 70, Hitachi), transmission electron microscopy (TEM, JEM-3010, JEOL). The concentration of components in SCSC was measured by energy dispersive spectra (EDS) attached with FETEM. An ultraviolet–visible spectrophotometer (UV 2,550, Shimadzu) were used to characterize the optical properties of samples.

Solar cell fabrication and measurements.

The thin film of Sn based nanomaterials was deposited onto ITO/glass substrate by spin-coating method at 3,000 rpm for 30 s, followed by drying on a hot plate at 150 ^{o}C for 5 min and repeated the procedure six times to control film thickness. After then, the perovskite layer was deposited onto the resulting each Sn-based film by a consecutive two-step spin coating process at 1,000 and 5,000 rpm for 10 and 20 s, respectively, from the mixture solution of methylammonium iodide (CH_3NH_3I) and PbI_2. The detailed preparation of the CH_3NH_3I has been described in our previous work. During the second step, toluene was dropped on the film to treat the morphology of perovskite film, and then was dried on a hot plate at 100 ^{o}C for 10 min. A solution poly(triarylamine) (EM index, Mn¼ 17,500 g/mol, 10mg in toluene 1 ml) was mixed with 15 ml of a solution of lithium bistrifluoromethanesulphonimidate (170 mg) in acetonitrile (1 ml) and 7.5 ml 4-tert-butylpyridine. The resulting solution was spin-coated on the $CH_3NH_3PbI_3$/Sn based ETL thin film at 3,000 rpm for 30 s. Finally, an Au counter electrode was deposited by thermal evaporation. Time-resolved photoluminescence (TRPL) curves were recorded using a commercial Time-Correlated Single Photon Counting (TCSPC) system (FluoTim 200, PicoQuant). Samples were photoexcited by picosecond diode laser of 670 nm (LDH-P-C-670, PicoQuant) with a variable repetition rate (1MHz) (since the reference was measured at 1Mhz). The emitted PL was spectrally dispersed with monochromater (ScienceTech 9030) for each PL signal, and was collected by a fast photon multiplier tube (PMT) detector (PMA 182, PicoQuant GmbH) with a magic angle (54.7°) arrangement. The incident angle of excitation pulse was set to be about 30° with respect to the sample. The resulting instrumental response function was about 160 ps in full-width-half-maximum. And all of the signals were measured at the emission peak (770±5nm) for perovskite. In addition, a cut-off filter (FF01-692nm, Semrock) was applied to block the remaining

scattering. Transient photovoltage decay measurement was performed using a nanosecond laser (pulsed 10 Hz, NT342A-10, EKSPLA) pumped OPO pulse of 550 nm and a Xe lamp (continuous wave, 150 W, Zolix) as an attenuated perturbation light pulse and a bias light source, respectively. The sample devices were electrically connected to a digital oscilloscope (500 MHz, DSO-X 3054A, Agilent) with BNC cables, and the input impedance was set to be 1 MΩ (Keithley 2001) for an open circuit condition. The bias light intensity was controlled by neutral density filters from 0.0 to 0.5 sun to vary open-circuit voltages (Voc). The *J–V* curves were measured using a sourcemeter (Keithley 2,420) and a solar simulator (Oriel Class A, 91,195 A, Newport) giving light AM 1.5 G illumination, and a calibrated Si-reference cell certified by the NREL. A metal mask with a circular aperture (0.096 cm^2) was applied on top of all devices. The step voltage and the delay time were fixed at 10 mV and 40 ms, respectively. The EQE was measured using a 300W xenon lamp (66,920, Newport) as a power source with a monochromator (Cornerstone 260, Newport) and a multimeter (Keithley 2001).

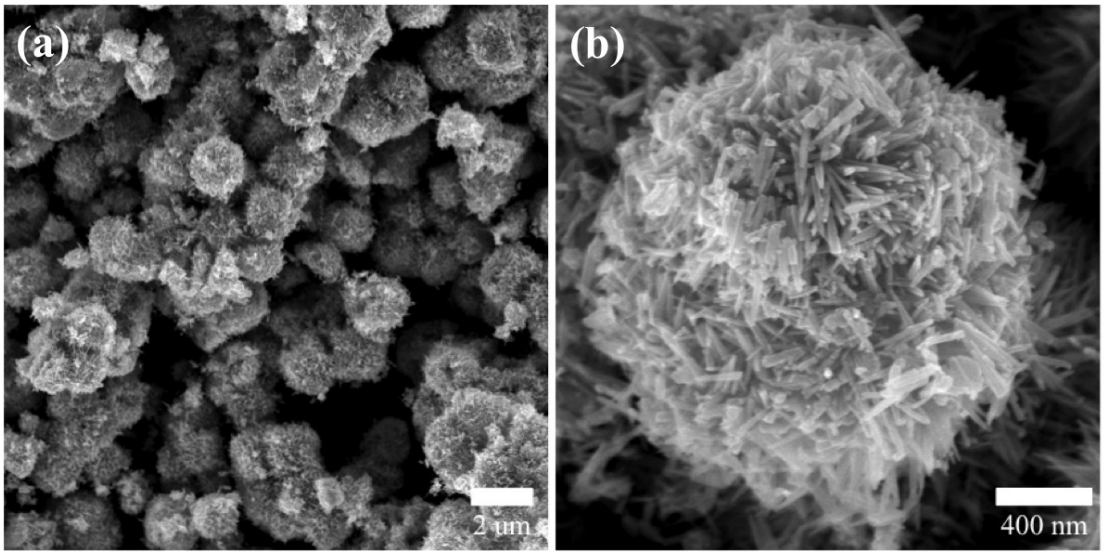

Figure S1. SEM image of Zn doped SnO_2 synthesized using NaOH as OH^- supplier instead of N_2H_4 at the low Zn/Sn molar ratio conditions: (a) Low-magnification SEM image, and (b) High-magnification SEM image

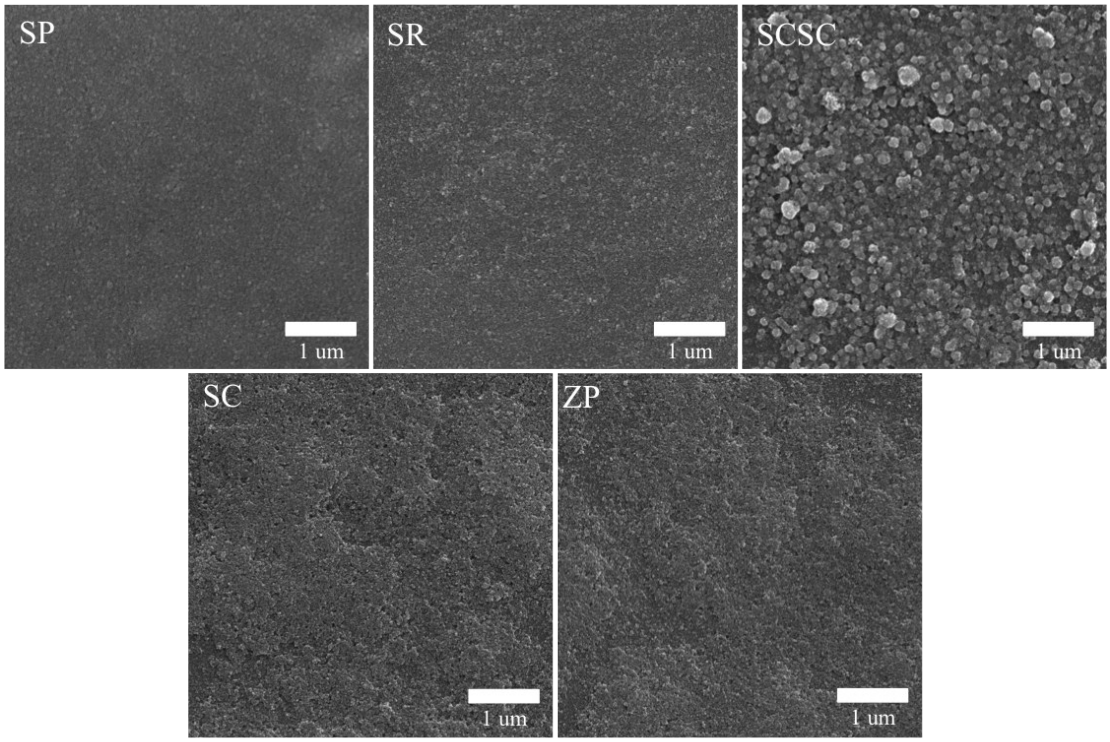

Figure S2. Plane-view SEM images of tin-based nanostructures film on fused silica substrates: (a) SP, (b) SR, (c) SCSC, (d) SC, and (d) ZP.

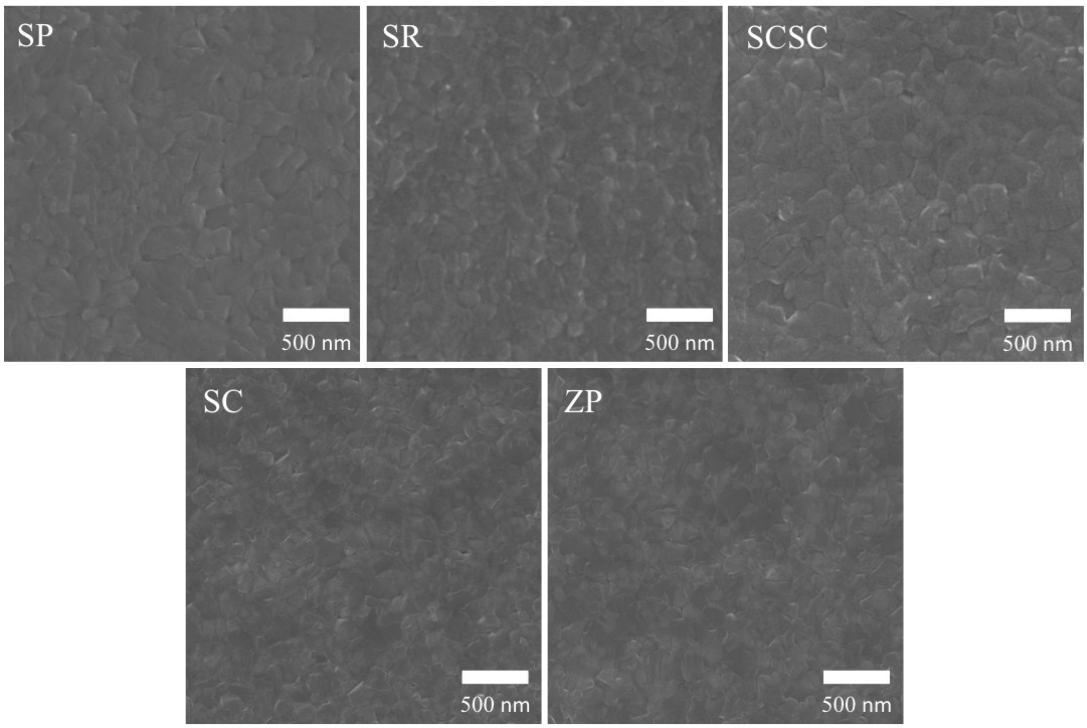

Figure S3. Plane-view SEM images of perocskite/ETL films on fused silica substrates: (a) SP, (b) SR, (c) SCSC, (d) SC, and (d) ZP.

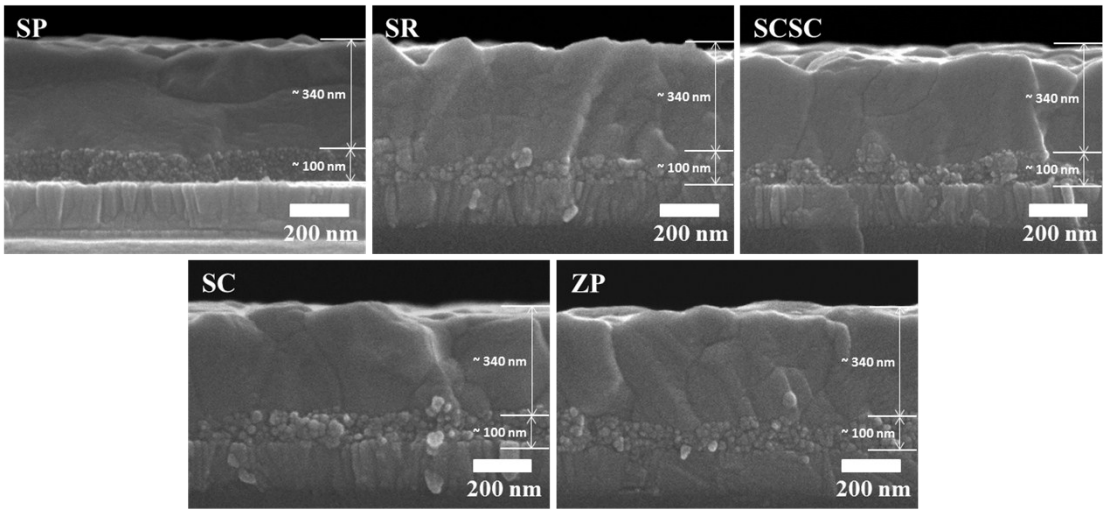

Figure S4. Cross-sectional SEM images of perocskite/ETL films on fused silica substrates: (a) SP, (b) SR, (c) SCSC, (d) SC, and (d) ZP.

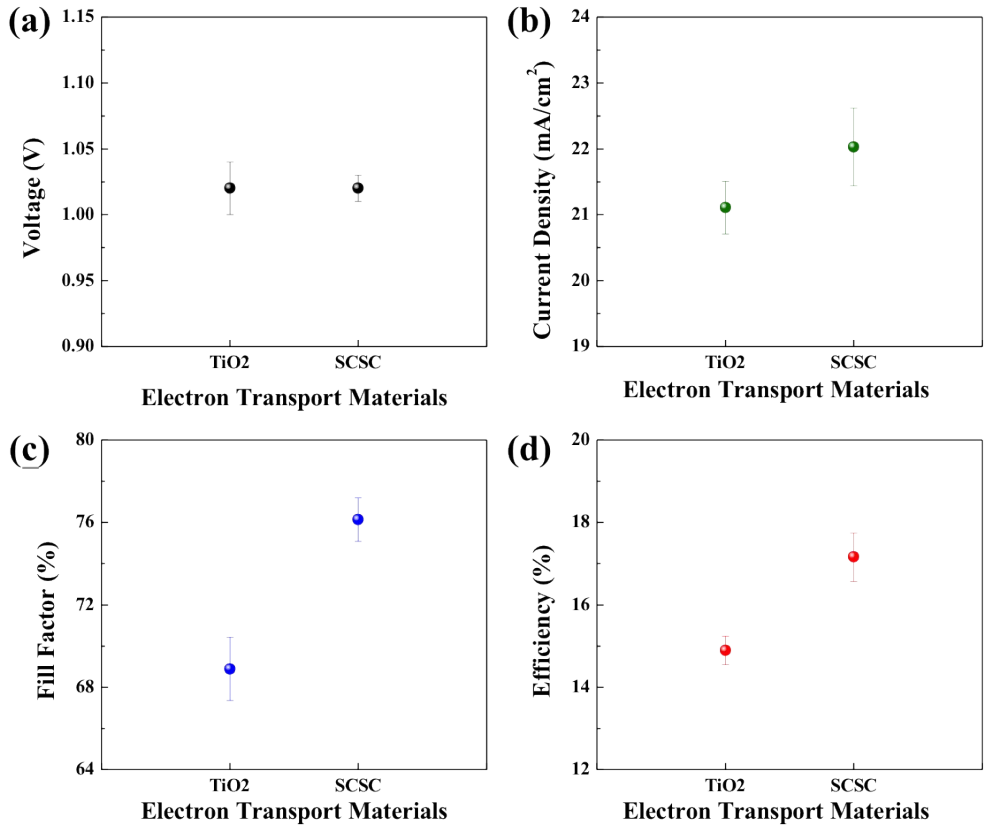

Figure S5. Average photovoltaic properties of TiO_2- and SCSC- based PSCs: (a) Open-circuit voltage (V_{oc}), (b) Photocurrent density (J_{sc}), (c) Fill factor (*FF*), and (d) Power conversion efficiency (□□ as a function of ETL, respectively.

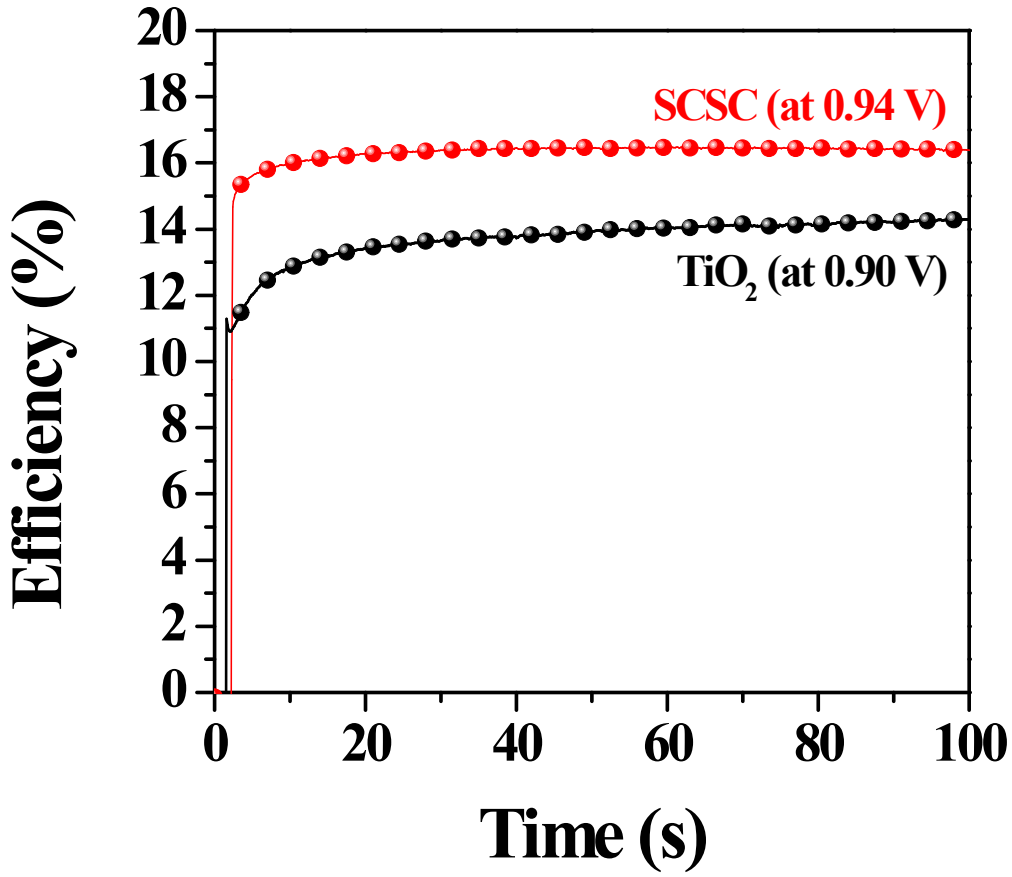

Figure S6. The stabilized power conversion efficiency of SCSC-based and TiO_2-based PSCs at the maximum power point, respectively (0.94 V and 0.90 V).

Table S1. Average photovoltaic parameters of TiO_2- and SCSC- based PSCs

Sample	V_{oc} (V)	J_{sc} (mA/cm^2)	*FF* (%)	η (%)
TiO_2	1.02 ± 0.02	21.11 ± 0.40	68.89 ± 1.53	14.86 ± 0.35
SCSC	1.02 ± 0.01	22.09 ± 0.68	76.37 ± 1.14	17.26 ± 0.72